Received: 4 December 2017 | Revised: 31 January 2018 | Accepted: 31 January 2018

DOI: 10.1111/pce.13166

ORIGINAL ARTICLE

WILEY Plant, Cell & Environment

UV-B radiation delays flowering time through changes in the PRC2 complex activity and miR156 levels in *Arabidopsis thaliana*

Marcela Dotto* | **María Sol Gómez** | **María Soledad Soto** | **Paula Casati**

Centro de Estudios Fotosintéticos y Bioquímicos, Universidad Nacional de Rosario, Rosario, Santa Fe 2000, Argentina

Correspondence
Paula Casati, Centro de Estudios Fotosintéticos y Bioquímicos, Universidad Nacional de Rosario, 2000 Rosario, Santa Fe, Argentina, Suipacha 570, Rosario, Santa Fe Province 2000, Argentina.
Email: casati@cefobi-conicet.gov.ar

Funding information
Fondo para la Investigación Científica y Tecnológica, Grant/Award Numbers: PICT 2013-268 and PICT 2015-157

Abstract

UV-B is a high-energy component of the solar radiation perceived by the plant and induces a number of modifications in plant growth and development, including changes in flowering time. However, the molecular mechanisms underlying these changes are largely unknown. In the present work, we demonstrate that Arabidopsis plants grown under white light supplemented with UV-B show a delay in flowering time, and this developmental reprogramming is mediated by the UVR8 photoreceptor. Using a combination of gene expression analyses and UV-B irradiation of different flowering mutants, we gained insight into the pathways involved in the observed flowering time delay in UV-B-exposed Arabidopsis plants. We provide evidence that UV-B light downregulates the expression of *MSI1* and *CLF*, two of the components of the polycomb repressive complex 2, which in consequence drives a decrease in H3K27me3 histone methylation of *MIR156* and *FLC* genes. Modification in the expression of several flowering time genes as a consequence of the decrease in the polycomb repressive complex 2 activity was also determined. UV-B exposure of flowering mutants supports the involvement of this complex in the observed delay in flowering time, mostly through the age pathway.

KEYWORDS

Arabidopsis, flowering time, H3K27me3, miR156, PRC2, UV-B, UVR8

1 | INTRODUCTION

Plants are constantly exposed to multiple environmental stimuli influencing their growth and development. One of the most important sources of energy and information is sunlight, which is fundamental for the photosynthetic process but also allows plants to perceive environmental changes, such as the cycling of the seasons, the time of the day, or the presence of competitors. Plants are able to sense quantitative and qualitative changes in light conditions through the absorption of different wavelengths by photoreceptors, which initiate the corresponding signal transduction pathways, allowing plants to modulate their growth and development accordingly (Perrella & Kaiserli, 2016; Wu, 2014). UV-B is a component of the solar spectrum located at the shortwave zone (280–315 nm), of which wavelengths between 290 and 315 nm can reach the earth surface. Different studies on plants exposed to UV-B radiation have demonstrated that, depending on the dose and the length of the exposure, UV-B can have effects both as a stressor and as a regulator of plant growth and development (Frohnmeyer & Staiger, 2003; Mackerness, 2000; Parihar, Singh, Singh, Singh, & Prasad, 2015). Stress responses occur mainly at high doses of UV-B in nonacclimated plants, whereas regulatory photomorphogenic effects take place at low levels of this radiation, allowing the acclimation of plants without signs of stress (Parihar et al., 2015; Vanhaelewyn, Prinsen, Van Der Straeten, & Vandenbussche, 2016). UV RESISTANT LOCUS 8 (UVR8) is the only UV-B specific photoreceptor identified (Jenkins, 2014; Rizzini et al., 2011), which has been shown to enhance Arabidopsis plant survival under low UV-B levels (Favory et al., 2009; Rizzini et al., 2011). These responses require the integration of different signalling pathways, which usually involve primary changes at the gene expression level, some of which have been shown to rely on UVR8 action (Casati, 2013; Casati & Walbot, 2003; Dotto & Casati, 2017). The most common effects of UV-B on plant physiology, growth, and development range from specific modifications on primary metabolic functions, such as a decrease in photosynthetic activity, changes in pigment composition, and enzyme activities, to more general effects such as the inhibition of cell proliferation (Casadevall, Rodriguez, Debernardi, Palatnik, & Casati, 2013), alterations in flowering time, and reproduction (Mackerness, 2000). Even though changes in flowering time in plants exposed to UV-B have been reported (Rajendiran & Ramanujam, 2004; Saile-Mark & Tevini, 1997),

*Facultad de Ciencias Agrarias, Universidad Nacional del Litoral, Esperanza, Santa Fe 3080, Argentina.

the underlying details leading to such changes are currently unknown, especially in Arabidopsis, where studies are largely missing.

The control of flowering time is crucial for reproductive success, as maximal pollination and seed set occur when environmental conditions are most favourable. In order to achieve the tight regulation of flowering, multiple pathways have evolved to integrate several environmental and endogenous cues (Battey, 2000; Marquardt, Boss, Hadfield, & Dean, 2006). Five flowering pathways have been characterized in the control of flowering time: photoperiod, vernalization, gibberellin, autonomous, and age pathways. All five pathways integrate endogenous and environmental signals and include the participation of numerous genes and complex genetic networks to guarantee the reproductive success and spread of seeds. Eventually, all these flowering pathways converge on a small number of so-called floral integrators: *FLOWERING LOCUS T* (*FT*), *SUPPRESSOR OF OVEREXPRESSION OF CONSTANS 1* (*SOC1*), and *LEAFY* (*LFY*). Once the expression of these integrators exceeds a threshold, plants initiate flowering, which is generally an irreversible process (Komeda, 2004; Moon, Lee, Kim, & Lee, 2005; Salomé, Bomblies, Laitinen, Yant, & Mott, 2011; Tooke, Ordidge, Chiurugwi, & Battey, 2005). The photoperiod pathway responds to seasonal changes in day length, and the vernalization pathway responds to prolonged exposure to cold. The autonomous and gibberellin pathways mediate the response to endogenous signals, being the gibberellin pathway especially important for plants growing under short-day conditions (Mutasa-Göttgens & Hedden, 2009; Simpson, 2004). Finally, the age pathway regulates juvenile to adult and vegetative to reproductive phase transitions as the plant matures (Hyun, Richter, & Coupland, 2016; Wang, 2014; Wu et al., 2009). In addition, light quality, ambient temperature, and biotic as well as abiotic stresses can contribute to floral induction in plants through the modulation of one or more of the flowering pathways (Cho, Yoon, & An, 2016; Simpson, 2004).

The growing conditions used in the present study were oriented to mimic, in laboratory conditions, one life cycle in a natural scenario, where plants grow under a long day setting and receive a daily dose of UV-B radiation within the order of magnitude perceived in a wild environment. Accordingly, the age and the autonomous pathways are of special interest for the present study. In the age pathway, the sequential action of miR156 and miR172 controls the timing of the juvenile to adult and the vegetative to reproductive transitions. Expression of miR156 is highest during young developmental stages and decreases gradually as plants mature, promoting the transition to the adult phase. An opposite pattern is observed for the accumulation of miR156 targets, the members of the *SQUAMOSA PROMOTER BINDING PROTEIN-LIKE* (*SPL*) family (Jung, Seo, Kang, & Park, 2011; Wang, Czech, & Weigel, 2009; Wu et al., 2009; Wu & Poethig, 2006). Members of this family, including *SPL9* and *SPL10*, promote the accumulation of miR172 through direct binding to the promoter of the precursor genes of this microRNA (Jung et al., 2011; Wang et al., 2009; Wu et al., 2009; Wu & Poethig, 2006). In turn, miR172 negatively regulates the flowering repressors *APETALA2*-like transcription factors, which include *APETALA2* (*AP2*); *TARGET OF EAT1* (*TOE1*), *TOE2*, and *TOE3*; *SCHNARCHZAPFEN* (*SNZ*); and *SCHLAFMÜTZE* (*SMZ*). In consequence, miR172 promotes the appearance of adult traits as well as flowering through downregulation of its targets (Aukerman & Sakai, 2003; Hyun et al., 2016).

The central integrator of the autonomous and vernalization pathways is *FLOWERING LOCUS C* (*FLC*), which is regulated by a number of proteins classified as the autonomous pathway, which include *FCA*, *FVE*, and *FLOWERING LOCUS D* (*FLD*). *FLC* represses flowering quantitatively through blocking the expression of the floral pathway integrators, *FT*, and *SOC1* (Michaels & Amasino, 1999; Sheldon et al., 2000).

The precise control of flowering time involves several gene regulatory mechanisms, including direct repression or activation of gene expression by transcription factors binding to promoter regions, posttranscriptional repression through miRNAs, and epigenetic modification at the chromatin level of several genes (Deng et al., 2011; Spanudakis & Jackson, 2014; Tooke et al., 2005). *FLC* is one of such genes whose regulation is under epigenetic control, decreasing gene expression through histone deacetylation by a complex containing *FVE*, as well as histone methylation by the polycomb repressive complex 2 (PRC2; Ausín, Alonso-Blanco, Jarillo, Ruiz-García, & Martínez-Zapater, 2004; De Lucia, Crevillen, Jones, Greb, & Dean, 2008; Simpson, 2004). By deposition of the repressive mark H3K27me3, the PRC2 complex also regulates flowering time through epigenetic regulation of *FT* and the transition to adult phase by targeting *MIR156* genes (Jiang, Wang, Wang, & He, 2008; Lopez-Vernaza et al., 2012; Xu, Hu, Smith, & Poethig, 2015).

In the present work, we analysed flowering time in Arabidopsis plants grown under a daily UV-B treatment. By use of gene expression analysis, chromatin immunoprecipitation (ChIP) followed by qPCR and UV-B irradiation of mutants in the age and the autonomous pathways, we demonstrate that UV-B radiation delays flowering time in *Arabidopsis thaliana* through downregulation of the expression of *CLF* and *MSI1*, two of the components of the PRC2 complex. These changes result in a decrease of the repressive H3K27me3 mark at *FLC* and *MIR156* chromatin, leading to an upregulation of the repressor of flowering *FLC*; an increase in the accumulation of miR156; and a global decrease in the expression of the floral integrators *FT*, *SOC1*, and *LFY*. However, changes in miR156 expression and the consequent modifications in the downstream regulatory pathway seem to be the major players for the observed late flowering phenotype after UV-B exposure. Moreover, irradiation of *uvr8* mutants and gene expression analysis of flowering genes in these mutant plants indicate that the effect of UV-B light on flowering time depends on this photoreceptor. Together, our results show that UV-B radiation delays flowering time by affecting gene expression of different members of the flowering pathways and the floral integrators, as a consequence of changes in the activity of the PRC2 complex, mainly through the regulation of the age pathway and the UVR8 photoreceptor.

2 | MATERIALS AND METHODS

2.1 | Plant material, growth conditions, and irradiation protocols

A. thaliana ecotype Col-0 was used for all experiments. The *35S::MIR156a*, *MIM156*, *spl9-4* and *toe1-2/toe2-1* seed stocks were provided by Dr. Scott Poethig (University of Pennsylvania, USA). The *clf-29* mutant (SALK_021003) was provided by Dr. Aman Husbands

(Timmermans Lab, CSHL, USA). The *flc-3* mutant and the *FRI flc-2* line were provided by Dr. Julia Questa (Caroline Dean Lab, JIC, UK). The *hyl1-2*, *se-1*, and *uvr8*-mutant lines were provided by Dr. Javier Palatnik (IBR, Rosario, Argentina); Dr. Nahuel González-Schain (IBR, Rosario, Argentina); and Dr. Roman Ulm (University of Geneva, Switzerland), respectively. The *msi1-5* (CS850909) seed stock was obtained from the ABRC stock centre. Plants were planted in soil, stratified for 3 days at 4 °C, and transferred to a growth chamber under long-day condition (16 hr light/8 hr dark) at 23 °C or short-day condition (8 hr light/16 hr dark) at 24 °C in a growth chamber (Adaptis A1000, Conviron). For the UV-B treatment, white light was supplemented with 2 Wm^{-2} of UV-B (311 nm; Phillips narrowband TL/01 lamps); during 1 hr every day starting from Day 9 after transferring to the growth chamber until flowering, the zeitgeber time of UV-B treatments was 4 hr in both long- and short-day conditions. The UV-B intensity used is similar to solar UV-B reaching Rosario, Argentina, at noon in summer time. As a no UV-B control, plants were exposed for the same time under the same lamps covered with polyester filters that absorb UV-B at wavelengths lower than 320 nm (PE, 100 mm clear polyester plastic; Tap Plastics). UV radiation was measured using a UV-B/UV-A radiometer (UV203 AB radiometer; Macam Photometrics). Samples were collected immediately after the light treatments. The UV-B treatments were started at 9 days because at this time point, the first true leaves are emerging, and this allows for the identification of plants in the same developmental stage. At 5–7 days, cotyledons have just emerged or are expanding; thus, at these days, it is usually difficult to assess plant developmental stage (Figure 1a).

2.2 | Determination of flowering time

Flowering time was counted as the number of rosette leaves at the moment of flowering or the number of days until the first flower opens, similar to previous reports (Koornneef, Hanhart, & van der Veen, 1991; Questa, Song, Geraldo, An, & Dean, 2016). Days were counted from the day of transfer to the growth chamber.

For the analysis of the *msi1-5/+* mutants, 30 seeds for each treatment (control and UV-B) from self-pollination of *msi1-5/+* mutants were planted. The flowering time for all of them was recorded as the number of rosette leaves at flowering and days to flowering. Afterwards, each plant was PCR genotyped using primers listed in Table S1, and only data for *msi1-5/+* mutants were used for analyses.

2.3 | RNA extraction and qRT-PCR

Total RNA was extracted from whole seedlings grown under long-day light conditions after 9th day of growth (immediately after the first day

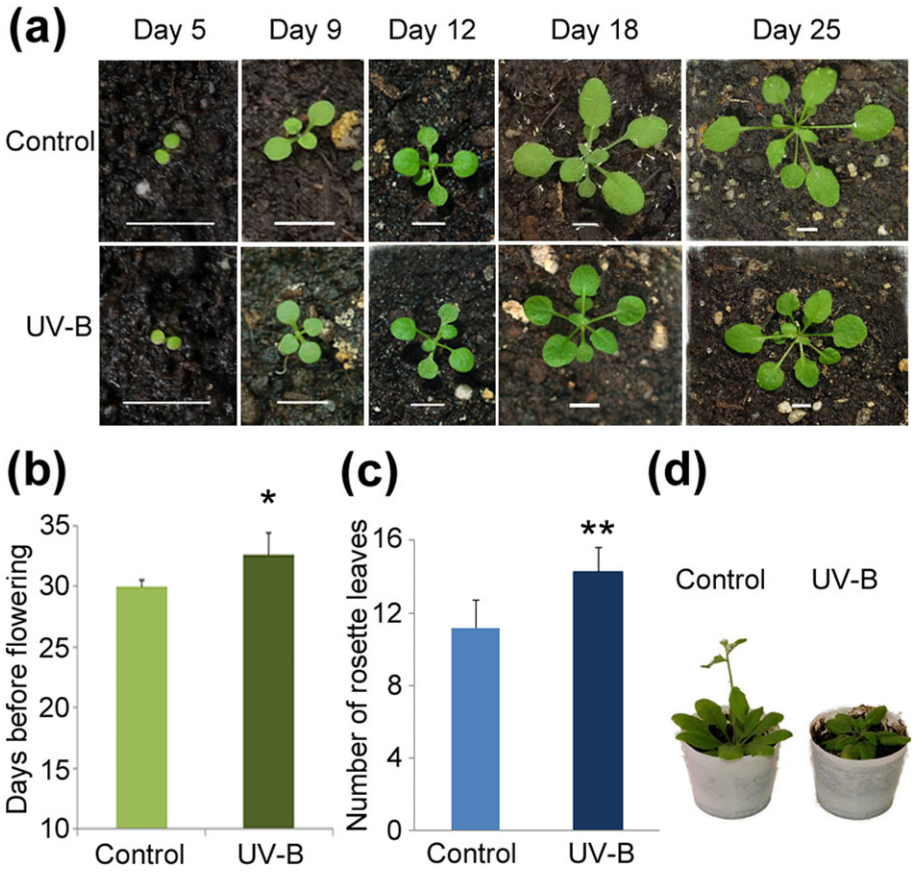

FIGURE 1 UV-B radiation delays flowering time. (a) Representative individual plants at the different time points during the development of control and UV-B irradiated plants. UV-B treatment starts at Day 9, when plants are developing the first true leaves. White bar = 0.5 cm. (b) Days before flowering in control plants compared with UV-B irradiated plants. (c) Number of rosette leaves in control plants compared to UV-B irradiated plants. (d) Picture of plants grown under white light supplemented with UV-B light, which flower later than control plants. Representative individuals are shown at 28 days of growth. (b–c) Values represented are mean ± SD across three biological replicates ($n \geq 10$ per replicate; Student's t test, * = $p < 0.05$; ** = $p < 0.001$) [Colour figure can be viewed at wileyonlinelibrary.com]

of UV-B treatment); the 12th day of growth (juvenile phase, before transition to reproductive growth); the 18th day of growth (adult phase); and the day of flowering of control plants (Figure 1a). RNA was isolated from 100 mg of pooled tissue using the TRIzol reagent (Invitrogen) according to manufacturer's instructions. Then, 2 μg of total RNA was incubated with RNase-free DNase I (1 unit/μL) following the protocol provided by the manufacturer (Promega), followed by reverse-transcription into first-strand cDNA using SuperScript II reverse transcriptase (Invitrogen), oligo(dT) and stem-loop oligos for miRNA156 and miR172 (Varkonyi-Gasic, Wu, Wood, Walton, & Hellens, 2007). The obtained cDNA was used as a template for quantitative PCR amplification in a Stratagene Mx3000P qPCR System (Agilent), using the intercalation dye SYBRGreen I (Invitrogen) as a fluorescent reporter and Platinum Taq polymerase (Invitrogen). Primers for each of the genes under study were designed or obtained from previous reports (Table S1). Amplifications were performed under the following conditions: 2 min of denaturation at 94 °C, 40 cycles at 94 °C for 15 s, 55 °C for 15 s, and 72°C for 30 s, followed by a 2 min extension at 72 °C. Three biological replicates and three technical replicates were performed for each sample. Melting curves for each PCR were determined by measuring the decrease of fluorescence with increasing temperature (from 65 to 98 °C). PCR products were run on a 2% (*w*/*v*) agarose gel to confirm the size of the amplification products and to verify the presence of a unique PCR product. Gene expression levels were normalized to that of Arabidopsis *CALCIUM DEPENDENT PROTEIN KINASE3* (*CPK3*) whose expression was previously reported to remain unchanged after UV-B irradiation (Ulm et al., 2004).

2.4 | Chromatin immunoprecipitation

For ChIP experiments, whole seedlings irradiated with UV-B for 4 days or kept under control conditions in the absence of UV-B were used. ChIP experiments were carried out as described in Casati et al. (2008). For each reaction, 4 μL of anti-H3 trimethylated K27 (ab6002) or anti-H3 (ab1791) antibodies was used (Abcam, Cambridge, MA). Two biological replicates from each sample were used. ChIP experiments were quantified by quantitative PCR (qPCR) in triplicates with appropriate primers (Table S1). For H3K27me3 analysis, data are represented as the ratio of H3K27me3/H3 to STM/H3.

2.5 | Statistical analysis

Statistical evaluations with Student's *t* test or ANOVA and graphical representation of the data were performed using the SigmaPlot software package and Microsoft Excel. The means and SE are derived from independent biological samples, unless otherwise stated.

3 | RESULTS

3.1 | UV-B radiation delays flowering time in *A. thaliana*

In order to investigate whether UV-B radiation affects Arabidopsis flowering time, we exposed plants to a daily dose of UV-B light for 1 hr at an intensity of 2 $W.m^{-2}$, starting at 9 days of growth, when plants are developing the first true leaves (Figure 1a). We observed that UV-B radiation delays flowering time indicated both by an increase in the number of days before flowering (Figure 1b) and by an increase in the number of rosette leaves in UV-B irradiated plants both under long and short days (Figures 1c and S1a). Representative control and UV-B treated wild-type Arabidopsis plants grown under long- and short-day conditions are shown in Figures 1d and S1b, respectively. For subsequent analyses, all experiments were done under long-day conditions, and the parameter days before flowering were used to analyse flowering time.

3.2 | Expression of *FT*, *SOC1*, and *LFY* is downregulated in plants exposed to UV-B radiation

Previous reports demonstrated that UV-B irradiation affects plant growth and development by changes in the expression of genes that regulate these processes (Casadevall et al., 2013; Casati, 2013; Casati & Walbot, 2003). To investigate whether the observed delay in flowering time is associated to changes in the expression of flowering regulators, we used qRT-PCR to compare gene expression levels of the floral integrators *FT* and *SOC1* and the floral identity gene and floral integrator *LFY* in control and UV-B exposed plants at different time points starting at 12 days, when plants are in the juvenile phase of vegetative growth, right before the transition to reproductive growth (Klepikova, Logacheva, Dmitriev, & Penin, 2015); at 18 days, when plants are in the adult phase transitioning to flowering; and at 25 days, the first bolting day of control plants (Figure 2a). *SOC1* was downregulated by UV-B light at 12 days, whereas *FT* and *LFY* were downregulated by this radiation both at 12 and 18 days. By the time control plants were bolting, *SOC1* and *LFY* expression was similar in UV-B treated and untreated plants, whereas *FT* expression remained downregulated in UV-B treated plants (Figure 2a). All these genes are central integrators of the different internal and environmental signals perceived by the plant through diverse flowering pathways, promoting flowering once their expression reaches certain threshold levels (Huijser & Schmid, 2011; Moon et al., 2005). Therefore, the observed downregulation in their expression correlates with the delay in flowering time measured after UV-B exposure.

3.3 | UV-B irradiation results in decreased H3K27me3 associated to flowering time genes

To gain insight into the mechanisms leading to the downregulation of the floral integrators after exposure to UV-B radiation, we analysed the effect of UV-B on the expression of selected members of the age pathway (miR156 and miR172) and the autonomous pathway (*FVE* and *FLC*), because these two pathways are likely to be important under the growing conditions used for the present study (Figure 2b,c). In addition, expression of *CONSTANS* (*CO*) was analysed as a component of the photoperiod pathway (Figure 2e). Finally, considering the regulation of flowering by the PRC2 complex occurs upstream of these flowering pathways, we also investigated if the expression of *MSI1* and *CLF*, as members of this complex, was also affected by this radiation (Figure 2d). Taking into consideration the developmentally regulated expression of miR156 (Wang et al., 2009; Wu & Poethig,

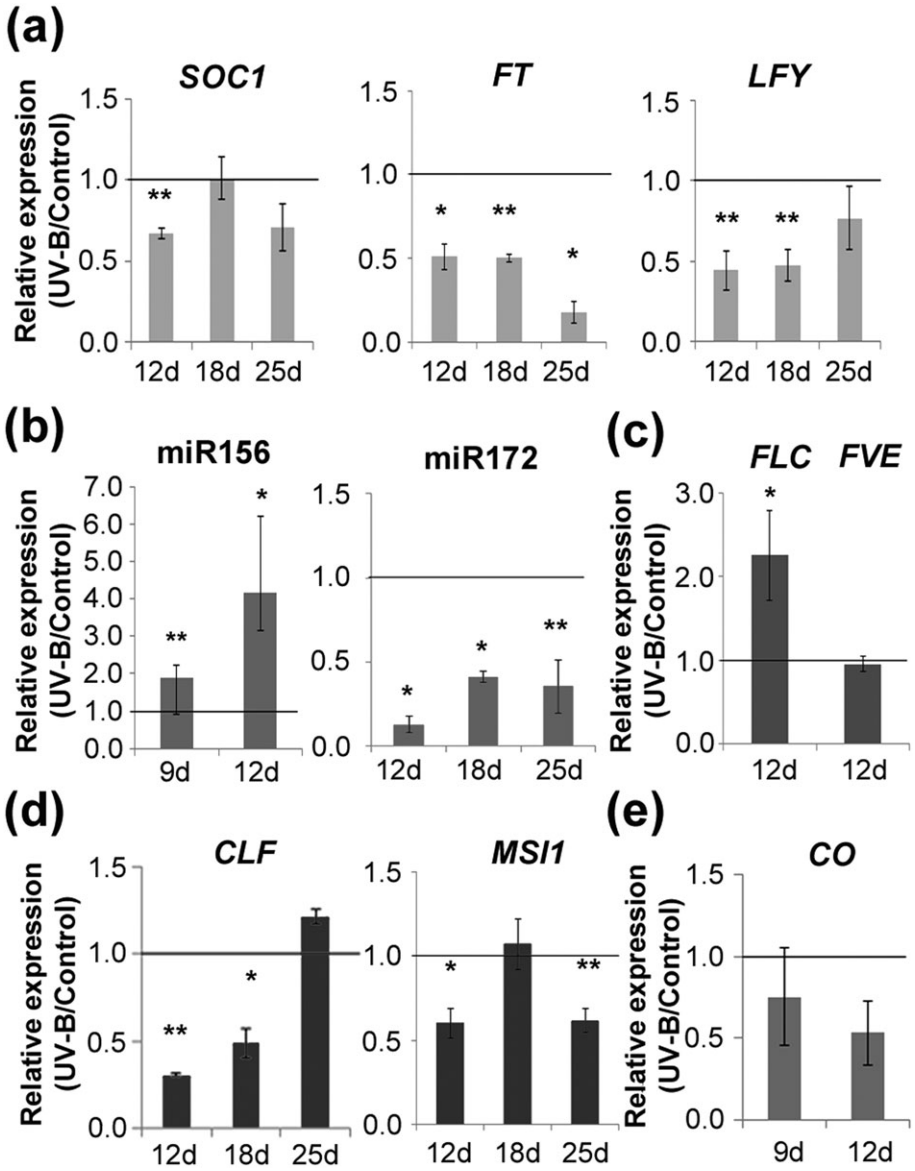

FIGURE 2 Changes in expression of flowering genes in UV-B exposed plants. (a) Relative expression of *SOC1*, *FT*, and *LFY* in control and UV-B irradiated plants analysed by qRT-PCR at different time points during development. (b) Relative expression of miR156 and miR172 in control and UV-B irradiated plants. (c) Relative expression of *FLC* and *FVE* in control and UV-B irradiated plants at 12 days. (d) Relative expression of *MSI1* and *CLF* in control and UV-B irradiated plants. (e) Relative expression of *CO* in control and UV-B irradiated plants. Transcript levels in UV-B treated plants normalized to untreated control plants are shown (mean ± *SD*; * = $p < 0.05$; ** = $p < 0.001$)

2006), we analysed the expression for this miRNA at 9 days of growth, which is immediately after initiation of UV-B exposure, and no further than 12 days of growth, because accumulation beyond this point is negligible. A similar decrease in expression has been reported for *FLC* (Klepikova et al., 2015); therefore, its expression was only analysed at 12 days of growth. Figure 2b shows that there is an increase in miR156 expression in irradiated plants at both time points analysed, whereas miR172 expression is downregulated by UV-B. On the other hand, the floral repressor *FLC* from the autonomous pathway is upregulated by UV-B at 12 days, whereas *FVE* and *CO* levels were not affected by the treatment (Figure 2c and 2e), suggesting that these genes do not have a role in the UV-B effect observed.

Interestingly, the expression of both *MSI1* and *CLF* was lower in plants exposed to UV-B than in control plants (Figure 2d). At 12 days, both genes are downregulated after UV-B exposure, whereas at 18 and 25 days, either *CLF* or *MSI1* accumulates at lower levels, respectively. Because they are members of the PRC2 complex, downregulation of one of them or both at the different time points analysed (Figure 2d) could affect PRC2 complex activity. To explore the possibility that the UV-B treatment could be influencing the activity of *SWINGER* (*SWN*), the alternative methyltransferase of the PRC2 complex, we also analysed the UV-B regulation of this gene. Our results showed that *SWN* expression is not affected by UV-B radiation under our experimental settings (Figure S2). Therefore, we explored whether a decrease in the expression of *MSI1* and *CLF* resulted in a differential deposition of the repressive mark H3K27me3 after UV-B exposure on the chromatin of the flowering genes known to be regulated by this complex. Thus, we performed ChIP on Arabidopsis control plants or daily exposed to UV-B and used qPCR to compare methylation levels for H3K27 associated to genes encoding two miR156 genes

(*MIR156A* and *MIR156C*), *FLC* and *FT*. We analysed changes in the association of this repressive mark to different regions in these genes that have already been documented to be associated to H3K27me3 (Figure 3). There was a significant decrease in the H3K27me3 levels associated to *MIR156C*, *FLC*, and one of the sites analysed for *MIR156A*, after UV-B exposure (Figure 3a,b), which correlates with the observed upregulation of miR156 and *FLC* by this radiation. However, the levels of H3K27me3 were unchanged at *FT* chromatin in UV-B treated plants.

3.4 | The response to UV-B irradiation of *clf-29* and *msi1-5* mutants supports the PRC2-mediated delay in flowering time

To gain further insight into the role of *MSI1* and *CLF* in the delay of flowering time in UV-B irradiated plants, we exposed *clf-29* and *msi1-5/+* mutants to the same UV-B treatment previously described. These flowering mutants have been described before and characterized in their role in flowering time (Jiang et al., 2008; Lopez-Vernaza et al., 2012; Steinbach & Hennig, 2014). Interestingly, we observed no difference in the flowering time of *msi1-5/+* heterozygous mutants that were exposed to UV-B light and the corresponding nonirradiated control (Figure 4a, Table S2), suggesting that in fact *MSI1* has a central role in the regulation of flowering time under UV-B conditions. Similarly, when *clf-29* mutants were grown under UV-B light, the delay in flowering time was not observed, presenting an early flowering phenotype compared to nonirradiated mutant plants (Figure 4a). Even though this result was unexpected, the number of rosette leaves in *clf-29* mutants remained unchanged in both control and UV-B conditions (Table S2), suggesting that the delay in flowering time in response to UV-B radiation requires the action of *MSI1* and *CLF*. Nonetheless, we analysed changes in expression of candidate genes that could explain the observed early flowering phenotype in irradiated mutants (Figure S3). In agreement with previous reports, *FT* and *FLC* expression is upregulated in *clf-29* mutants compared with Col-0 plants (Figure S3a; Jiang et al., 2008), whereas *SOC1* is downregulated in *clf-29* mutants (Figure S3a). Upon UV-B treatment, both *FT* and *SOC1* expression remained downregulated in *clf-29* mutant background (Figure S3b). Interestingly, as opposed to our results in Col-0 plants, *FLC* expression is downregulated after UV-B exposure, suggesting that this change in expression levels could be the cause of the early flowering phenotype observed in *clf-29* mutants. On the other hand, it is interesting to note that in our experiments, the flowering time under control conditions of *clf-29* mutants, measured by counting days before flowering, is similar as flowering time in WT plants, in contrast to what was previously reported (Jiang et al., 2008). However, when flowering time was analysed by counting the rosette leaves before flowering, *clf-29* flowered earlier than WT plants as previously reported (Table S2). Even though these two parameters usually correlate, in some rare cases, they do not (see, e.g., Xu et al., 2016). These differences may be due to experimental conditions.

To understand the consequences of the differential PRC2 complex activity after UV-B exposure, we initially investigated the role of FLC in the observed delay in flowering time. Therefore, we analysed the effect of UV-B radiation on *flc-3* mutant plants. According to previous reports, *flc-3* mutants flower earlier than Col-0 plants under control conditions (Michaels & Amasino, 1999; Figure 4b). However, and similarly to UV-B exposed Col-0 plants, *flc-3* mutants also flowered later than the untreated control plants (Figure 4b). One of the most important regulators of *FLC* is FRIGIDA (FRI), responsible for *FLC* activation to delay flowering during long vernalization periods (Sheldon et al., 2000; Shindo et al., 2005). Considering that the *fri* allele is not active in the Col-0 ecotype, a *FRI flc-2* line was also UV-B irradiated to test whether the FLC role in flowering time in response to UV-B light might be conditioned to the presence of FRI (Michaels & Amasino, 1999; Figure 4b). In agreement to previous reports, *FRI flc-2* plants flowered at the same time as Col-0 plants, because the *flc-2* mutation suppresses the late flowering phenotype determined by the introgression of the *FRI* allele. Similarly as observed for *flc-3* and Col-0 plants, *FRI flc-2* plants flowered later after the UV-B treatment (Figure 4b).

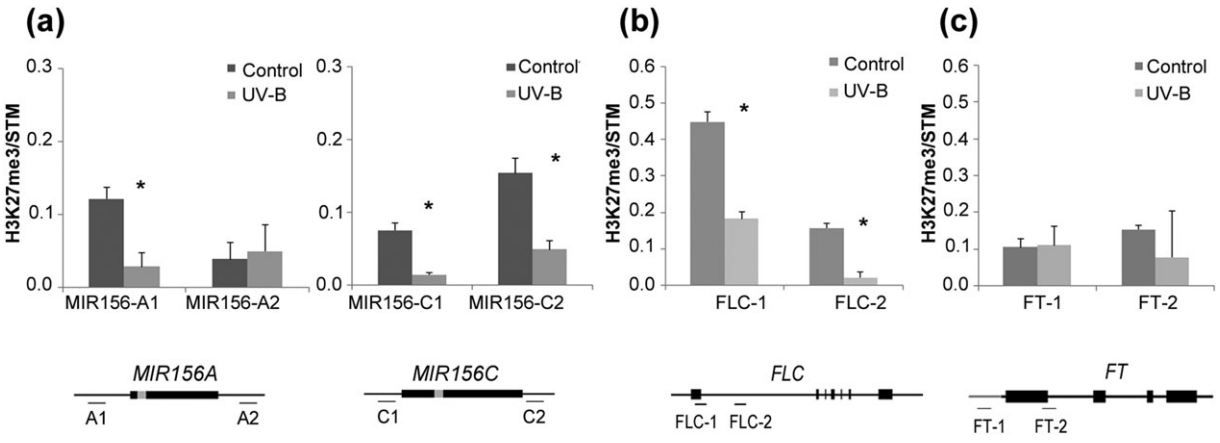

FIGURE 3 Effect of UV-B light on gene expression and H3K27me3 status of selected flowering-related genes. Chromatin immunoprecipitation (ChIP)-qPCR analyses of H3K27me3 in UV-B irradiated and control Col-0 plants at 12 days of growth. (a) H3K27me3 at *MIR156A* and *MIR156C*. Data are presented as the ratio of *MIR156A/H3* to *STM/H3* and *MIR156C/H3* to *STM/H3*. (b) H3K27me3 at *FLC*. Data are presented as *FLC/H3* to *STM/H3*. (c) H3K27me3 at *FT*. Data are presented as *FT/H3* to *STM/H3*. A scheme representing gene structure for *MIR156A* and *MIR156C*, *FLC* and *FT*, and the location of the PCR fragments amplified in ChIP-qPCR experiments are shown below each graphic (A1 and A2 for *MIR156A*; C1 and C2 for *MIR156C*); FLC-1 and FLC-2 for *FLC*; FT-1 and FT-2 for *FT*). Values are mean ± *SE* for two biological replicates, * = $p < 0.05$

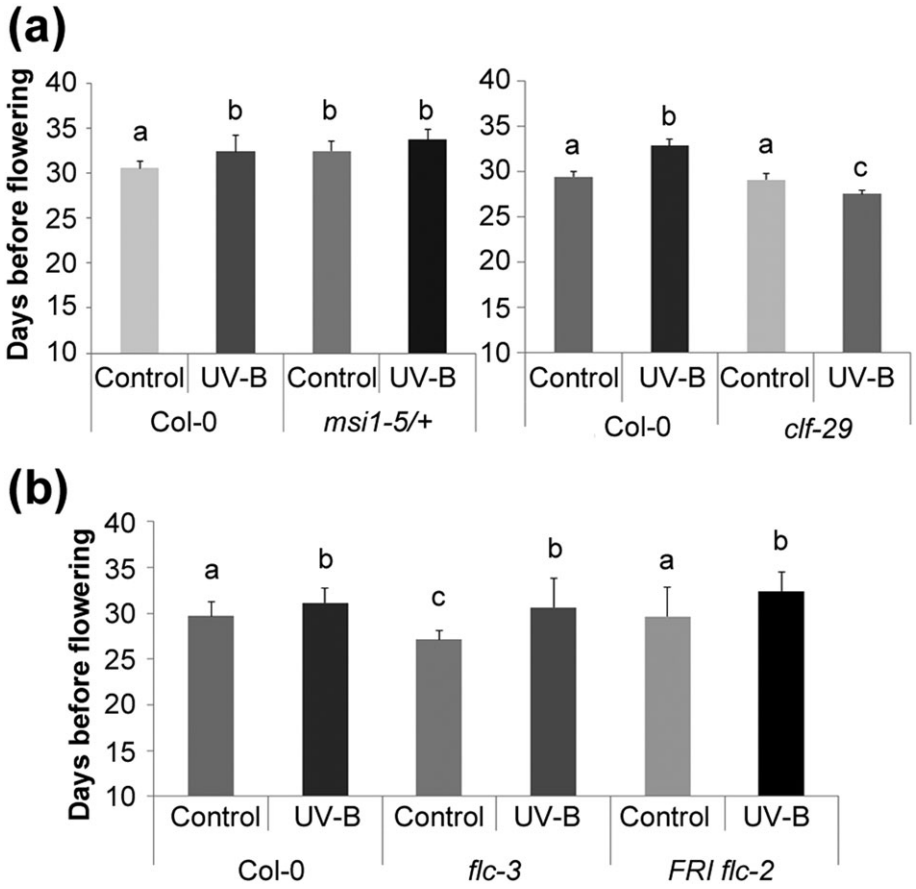

FIGURE 4 UV-B radiation on *msi1-5/+*, c*lf-29*, and *flc* mutants. (a) Days before flowering of control and UV-B treated *msi1-5/+*, *clf-29*, and Col-0 plants. (b) Days before flowering of control and UV-B treated Col-0, *flc-3*, and *FRI flc-2* plants. Values represented are mean ± SD; different letters indicate statistical difference (ANOVA, Fisher's LSD, $p < 0.05$; $n \geq 10$)

Altogether, these results suggest that despite the PRC2 mediated change in H3K27me3 at the *FLC* locus, the observed delay in flowering time after UV-B exposure seems to be subordinated to a different pathway.

3.5 | Decreased H3K27me3 on *MIR156* genes delays developmental phase transitions

To investigate a different downstream pathway affected by the reduced activity of the PRC2 complex after UV-B exposure, we looked into the role of the age pathway, which regulates transitions from juvenile to adult and vegetative to reproductive phases through the sequential action of miR156 and miR172 and their corresponding targets (Wang, 2014; Wang et al., 2009;Wu et al., 2009 ; Wu & Poethig, 2006). The appearance of abaxial trichomes is one of the first adult traits detected on rosette leaves, indicating the transition from juvenile to adult phase is occurring (Wu et al., 2009; Wu & Poethig, 2006). Thus, we analysed whether UV-B radiation caused an extended juvenile phase through the higher accumulation of miR156. Interestingly, we observed that the appearance of the first abaxial trichome was delayed from Leaf 6 (6.3 ± 0.45) in control plants to Leaf 8 (8.4 ± 0.5) in UV-B irradiated plants (Figure 5a), suggesting that the juvenile phase is indeed extended as a consequence of exposure to UV-B light. Thus, we then analysed the expression of *SPL9* and *SPL10*, two of the 11 miR156 targets, and *AP2*, *TOE1*, and *TOE2*, three of the six AP2-like targets of miR172 (Figure 5b; Hyun et al., 2016). *SPL9* and *SPL10* were downregulated in UV-B-treated plants, most likely as a consequence of the higher accumulation of mature miR156 (Figure 5b). On the other hand, miR172 targets were not affected by the treatment (Figure 5b), even when miR172 accumulated at lower levels in these plants (Figures 2b and 5b). However, the regulation of gene expression by miR172 is mostly translational in plants (Aukerman & Sakai, 2003); thus, it is possible that protein levels of these targets are still higher in UV-B exposed plants.

Next, we exposed *spl9-4* and *toe1-2/toe2-1* mutants to the daily dose of UV-B light previously described. Previous studies have shown that mutants in *spl9* show no difference in flowering time compared with wild-type plants, whereas the double mutant *toe1-2/toe2-1* presents an early flowering phenotype (Aukerman & Sakai, 2003; Schwarz, Grande, Bujdoso, Saedler, & Huijser, 2008; Xu et al., 2016). As expected, we observed these differences in flowering time when compared to Col-0 plants under control conditions in the absence of UV-B (Figure 5c,d). However, similar to Col-0 plants, a delay in flowering time by UV-B was observed in both mutant lines (Figure 5 c,d). Considering *SPL9* is only one out of 11 targets of miR156, and miR172 targets four other genes besides *TOE1* and *TOE2*; functional redundancy may occur in the response to UV-B for these transcription factors. Afterwards, we exposed plants from a *35S::MIR156a*

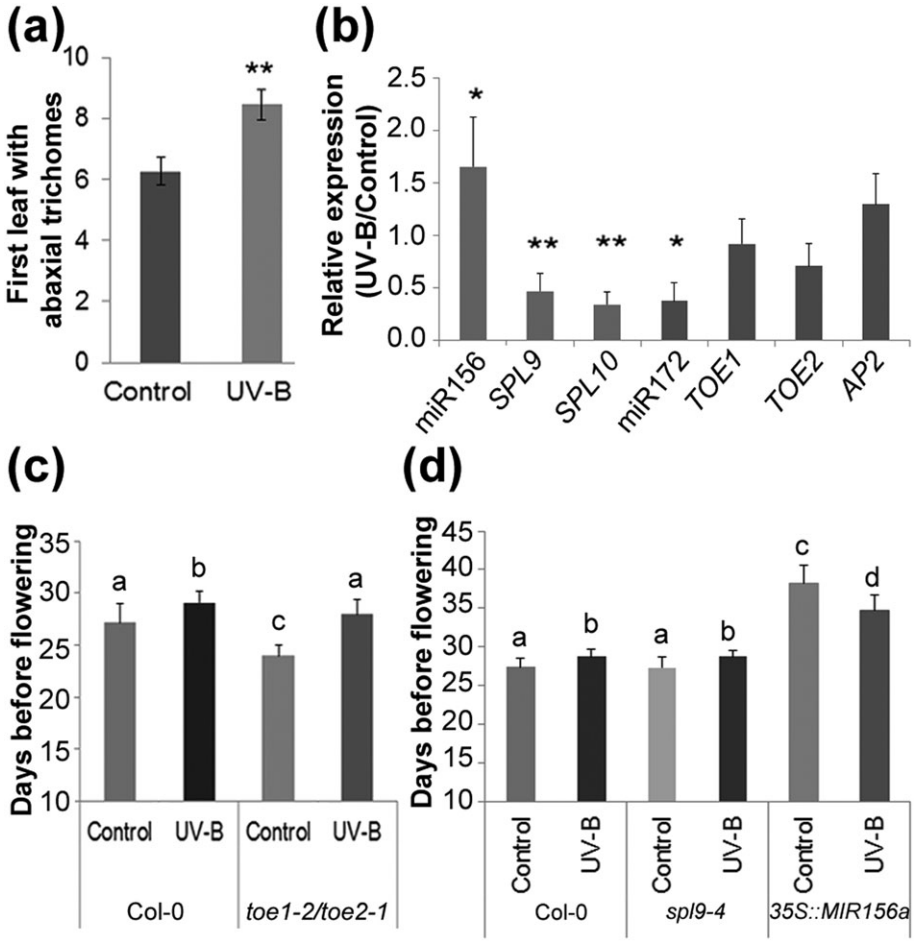

FIGURE 5 Effect of UV-B radiation on the age pathway. (a) Appearance of abaxial trichomes in UV-B exposed plants and nontreated control Col-0 plants. Values represented are mean ± *SD* ($n \geq 20$; Student's *t* test * = $p < 0.05$; ** = $p < 0.001$). (b) Relative expression of miR156, *SPL9*, *SPL10*, and miR172, *TOE1*, *TOE2*, and *AP2*, in control and UV-B irradiated plants. Analysis by qRT-PCR was performed at 9 days of growth for miR156 and its targets and at 12 days of growth for miR172 and its targets. Transcript levels in UV-B-treated plants normalized to untreated control plants are shown. (mean ± *SD*, * = $p < 0.05$; ** = $p < 0.001$). (c) Days before flowering of control and UV-B treated for *toe1-2/toe2-1* mutant and Col-0 plants. (d) Days before flowering of control and UV-B treated for Col-0 plants, *spl9-4* mutant and *35S::MIR156a* plants. Values represented are mean ± *SD*; different letters indicate significant difference (ANOVA, Fisher's LSD, $p < 0.05$; $n \geq 10$)

overexpression line to UV-B radiation. These plants were previously shown to have an extended juvenile phase and a late flowering phenotype as a consequence of the constitutive accumulation of miR156 along development (Wu et al., 2009). Interestingly, in UV-B exposed *35S::MIR156a* plants, the late flowering phenotype was reverted to a surprising early flowering phenotype compared to non-irradiated plants similar to that observed in *clf-29* mutants (Figure 5 d), indicating that the UV-B induced change in miR156 expression and the consequent modifications in the downstream regulatory pathway are necessary for the observed late flowering phenotype in Col-0 plants. The experiments were repeated using a *MIM156* line, which overexpresses a transgene harboring miR156 binding site that sequesters mature miR156. In agreement with previous results, these plants flowered very early (Huijser & Schmid, 2011) both under control and after UV-B exposure, and similar to the results using *35S::MIR156a* plants, they did not show a significant delay in flowering time by UV-B (Table S2).

Finally, in order to study whether the UV-B effect is related to changes in the biogenesis pathway of miR156 and/or miR172, we performed UV-B treatments on *se-1* and *hyl1-2* mutants. The delay in flowering time caused by UV-B light was also observed in both mutants (Figure S4), suggesting that the molecular mechanisms behind this developmental reprogramming do not involve changes in miRNA biogenesis.

3.6 | UV-B-induced delay in flowering time depends on the UVR8 signalling pathway

Finally, to analyse whether the UVR8 photoreceptor is involved in the delay in flowering time caused by UV-B radiation, we analysed flowering time in *uvr8* mutants (Figure 6a). Interestingly, *uvr8* mutant plants showed a late flowering phenotype when compared with Col-0 plants when they were grown in the absence of UV-B, but these mutants did not show a delay in flowering time after UV-B exposure, demonstrating that the observed delay in flowering time requires the activity of this photoreceptor (Figure 6a). Moreover, the expression of *CLF* and *MSI1* was unaffected by UV-B light in *uvr8* mutants (Figure 6b). Similar results were observed for *FLC*, miR156, and *SOC1* (Figure 6c–e), whereas the expression of *FT* was higher in irradiated plants after the first day of treatment but remained unchanged

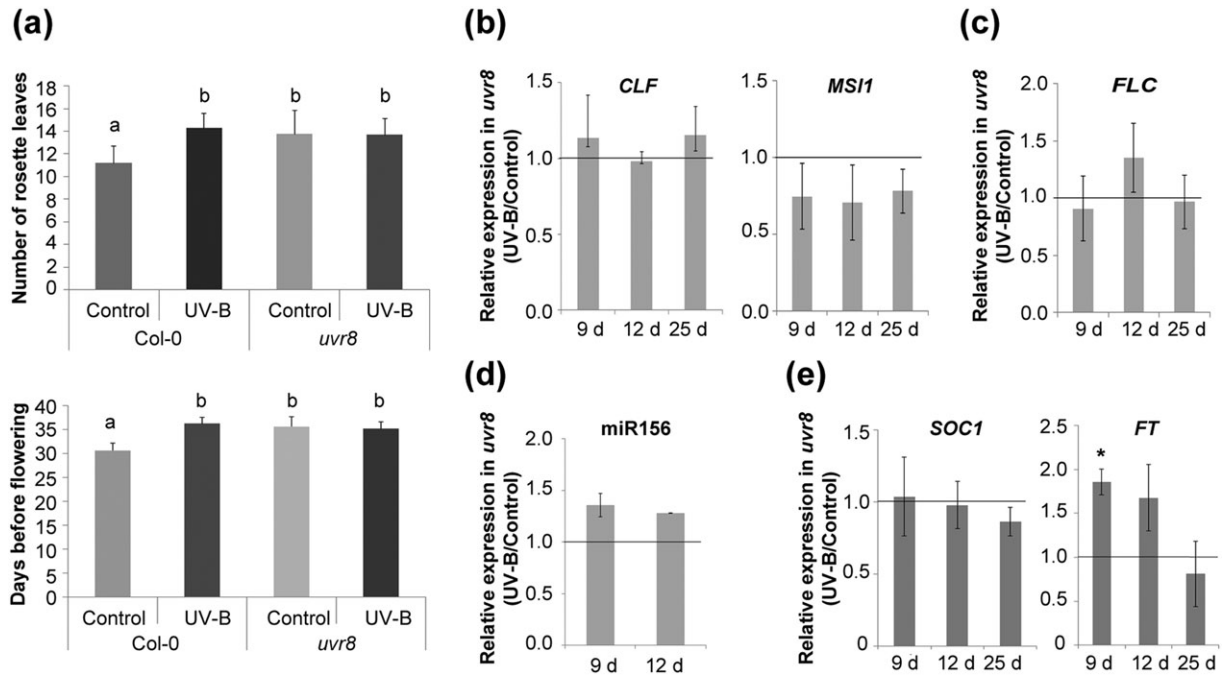

FIGURE 6 Dependence on UVR8. (a) Number of rosette leaves and days before flowering in control plants compared with UV-B irradiated plants, for wild-type (Col-0) and *uvr8* mutant plants. Values represented are mean ± *SD*; different letters indicate significant difference (ANOVA, Fisher's LSD, $p < 0.05$; $n \geq 10$). (b–e) Relative expression of flowering time genes in control and UV-B irradiated *uvr8* mutant plants analysed by qRT-PCR at different time points during development: (b) *CLF* and *MSI1*; (c) *FLC*; (d) miR156; and (e) *SOC1* and *FT*. Transcript levels in UV-B treated plants normalized to untreated control plants are shown (mean ± *SD*; * = $p < 0.05$; ** = $p < 0.001$)

afterwards (Figure 6e). It is important to note that not only UVR8 modulates UV-B responses in plants but also multiple molecular pathways are involved in plant responses to this radiation. These non-specific UV-B stress pathways include DNA damage signalling and defence and wound signalling pathways and MAP kinase activity, reactive oxygen species, and hormone signalling (Jenkins, 2017). Therefore, upregulation of *FT* by UV-B at Day 9 may be mediated by one or some of these other pathways. Altogether, these results demonstrate that UVR8 regulates the observed delay in flowering time by UV-B light in Arabidopsis.

4 | DISCUSSION

The correct timing of the transition to flowering is of outstanding importance, as it may have a strong impact on plant fitness. Flowering should occur when the environmental conditions are suitable and sufficiently reliable to allow completion of the process with the successful dispersal of seeds. For example, premature flowering usually results in reduced biomass and seed set. Similarly, prolonged vegetative growth might lead to an increase in biomass but, at the same time, often result in reduced seed number and seed filling (Demura & Ye, 2010; Huijser & Schmid, 2011). Previous reports indicated that UV-B radiation delays flowering time in some species (Rajendiran & Ramanujam, 2004; Saile-Mark & Tevini, 1997), but no mechanistic details have been described for these observations.

In our experimental settings, we found a delay in flowering time in UV-B exposed plants (Figures 1 and S1) and a concomitant downregulation in the expression of the three floral integrators *FT*, *SOC1*, and *LFY* (Figure 2a). These genes are central components of the complex genetic network involved in the control of flowering time, integrating endogenous signals, and environmental stimuli canalized by the different flowering pathways. It is interesting that although *SOC1* was only downregulated by UV-B light in 12 days samples, *FT* expression was clearly downregulated at 12, 18, and 25 days. One possible explanation for this is that both *SOC1* and *FT* are downregulated at 12 days, when plants are about to transition to reproductive phase. This decrease in expression could be sufficient for the developmental reprogramming to occur. Moreover, because *FT* expression is decreased after this time point, the accumulation of *FT* transcript might be lower than the threshold required to activate *SOC1* expression.

The autonomous and vernalization pathways converge at *FLC*, a flowering repressor whose expression decreases after prolonged exposure to cold temperature or as a consequence of the regulation through the components of the autonomous pathway (Deng et al., 2011; Marquardt et al., 2006). Because the growing conditions in the present work did not include vernalization, we chose to analyse *FVE* as a member of the autonomous pathway known to regulate *FLC* expression. *FVE*, also called *MSI4*, functions as part of several complexes to regulate epigenetically the expression of flowering genes by histone deacetylation (Ausín et al., 2004; Yu, Chang, & Wu, 2016). We observed upregulation of *FLC* expression in UV-B treated plants, but no difference in *FVE* expression was detected (Figure 2c). Also unchanged was the accumulation of *CO*, one of the members of the photoperiod pathway, as a consequence of UV-B treatment (Figure 2 e). Even though analysis of additional zeitgeber time points is necessary, this result suggests that the delay of flowering time by UV-B could be independent of clock genes. *FLC* is also subject to regulation

by the PRC2 complex, responsible for the downregulation of gene expression by deposition of the repressive mark H3K27me3 (De Lucia et al., 2008; Jiang et al., 2008; Lopez-Vernaza et al., 2012). When we analysed expression of *CLF* and *MSI1*, two of the components of this complex, we found that they were both downregulated in plants after UV-B irradiation (Figure 2d). Interestingly, *SWN* gene expression was not affected by this radiation (Figure S2), indicating that CLF is the key methyltransferase mediating this UV-B response. Using ChIP-qPCR, we found decreased H3K27me3 at previously reported sites on *FLC* (Figure 3b), indicating that the observed increase in *FLC* levels by UV-B could be a consequence of decreased PRC2 activity in plants grown under UV-B influence. In spite of the unchanged level of H3K27me3 at the *FT* locus (Figure 3c), the expression of this gene was downregulated in UV-B treated plants (Figure 2a), suggesting that an alternative way of regulation of *FT* is directly or indirectly affected by UV-B radiation. One possibility is that the direct repression of *FT* expression by UV-B-induced *FLC* bound to its first intron (Helliwell, Wood, Robertson, James, & Dennis, 2006) is responsible for the lower accumulation of *FT* mRNA.

Further implication of the regulation by PRC2 on the flowering time response to UV-B radiation comes from irradiation of *clf-29* and *msi1/+* mutants (Figure 4a). Homozygous *msi1* mutants are lethal; therefore, we analysed *msi1-5/+* heterozygous plants, which have been reported to present a late flowering phenotype (Steinbach & Hennig, 2014). Our results showed that *msi1-5/+* plants grown under UV-B flowered at the same time as the nonirradiated plants (Figure 4a, Table S2). Similarly, UV-B-treated *clf-29* mutants reversed the late flowering phenotype, presenting a surprising early flowering behaviour (Figure 4a, Table S2), which may be a consequence of *FLC* downregulation after UV-B exposure in this mutant background (Figure S3b). Thus, when we explored the role of downstream pathways affected by the differential accumulation of H3K27me3 at the chromatin level after UV-B exposure, we found that neither FLC nor its regulator FRI had a prevailing role in the delay in flowering time observed after UV-B exposure (Figure 4b). The role of FRI as a regulator of FLC has been mainly assessed in vernalized plants; because our experimental settings did not involve vernalization, the flowering behaviour of the *FRI flc-2* plants exposed to UV-B is not surprising. *flc-3* mutants also displayed a similar delay in flowering time as wild-type plants after UV-B exposure (Figure 4b), even when deposition of H3K27me3 was decreased (Figure 3) and *FLC* expression was upregulated after UV-B exposure (Figure 2b), suggesting that the role of FLC in the delay in flowering time after UV-B exposure may be subordinated to a different pathway. Interestingly, histone methylation by the PRC2 complex also participates in the age-dependent downregulation of *MIR156* genes (Xu et al., 2015). ChIP-qPCR also detected decreased H3K27me3 at the reported sites on *MIR156A* and *MIR156C* precursor genes after UV-B treatment (Figure 3a), suggesting that the observed increase in miR156 accumulation could be related to the decreased PRC2 activity in plants grown under UV-B influence (Figures 2b–d and 3a) and not due to changes in miR156 biogenesis (Figure S4). Gene expression analysis of selected members of the age pathway showed that the decreased expression of the floral integrators could also be a consequence of modifications in the expression of some of the genes in this pathway (Figures 2b,c and 5b). We found that the accumulation of mature miR156 and the decreased expression of two of its targets, *SPL9* and *SPL10*, is extended during development of UV-B exposed plants (Figure 5b), causing a delay in the transition to the adult phase, as evidenced by the late appearance of abaxial trichomes (Figure 5a). As a consequence, UV-B treated plants present a lower accumulation of mature miR172, whereas the analysed targets regulated by this miRNA did not show altered expression in plants grown under UV-B influence (Figure 5b). It is worth to mention that the regulation of *AP2*, *TOE1*, and *TOE2* by miR172 has been proposed to occur mainly at the level of translation (Aukerman & Sakai, 2003); therefore, unchanged transcript levels are not unexpected. In addition, differential expression of the repressors *TOE3*, *SNZ*, or *SMZ* supporting the observed delay in flowering time cannot be excluded. The involvement of the age pathway was also examined by exposing *spl9-4* and *toe1-2/toe2-1* mutant lines to UV-B radiation. In spite of the observed change in *SPL9* gene expression, a similar delay in flowering time was observed in *spl9-4* as in Col-0 plants exposed to UV-B radiation (Figure 5d). The *SPL* family is composed by 18 genes, 11 of which are targeted by miR156. Even though certain functional specification exists in adult traits formation, promotion of juvenile to adult, or the flowering transition, this is a highly redundant gene family as evidenced by the mild phenotype exhibited by single mutants (Huijser & Schmid, 2011; Hyun et al., 2016). Thus, a functional redundancy between *SPL9* and other members of the family may be the reason why the flowering response of *spl9-4* mutants under UV-B light was similar to that of WT plants. Similarly, UV-B irradiation of *toe1-2/toe2-1* mutants also resulted in late flowering (Figure 5c), which may be a result of other miR172 targets compensating for the absence of the mutated genes upon UV-B exposure. However, when we exposed *35S::MIR156a* overexpression lines to UV-B radiation, the delay in flowering time was reverted, resulting in an early flowering for irradiated plants compared with the corresponding control plants, similarly to *clf-29* mutants (Figure 5d). These results suggest that the effect of the PRC2 differential activity on the chromatin of *MIR156* genes affects the expression of members of the age pathway, leading to the regulation of flowering time under UV-B conditions.

The early flowering phenotype observed for *35S::MIR156A* and *clf-29* after UV-B radiation might be reflecting hierarchical layers of gene regulation that are affected by UV-B. For example, *FLC* regulation in a wild-type background occurs mainly at the chromatin level by PRC2 histone methylation (Jiang et al., 2008), and our results demonstrate that UV-B radiation causes an increase in *FLC* expression in this context (Figure 2c). However, when PRC2 regulation is eliminated in a *clf* mutant background, our data show that an alternative regulation of *FLC* is affected by UV-B, and a downregulation of this gene is observed (Figure S3b). This hypothesis requires further investigation in order to characterize this response.

Finally, the results presented here also demonstrate that UVR8, the UV-B photoreceptor, regulates the observed delay in flowering time by UV-B light by regulating the expression of flowering genes after exposure. In the UVR8 signalling cascade, CONSTITUTIVELY PHOTOMORPHOGENIC1 (COP1) acts as a positive regulator of responses to UV-B (Jenkins, 2017). When UVR8 and COP1 interact, transcriptional activation of several UV-B responsive genes occur, in particular *HY5* and *HYH* expression is activated (Favory et al., 2009). HY5 is the major effector

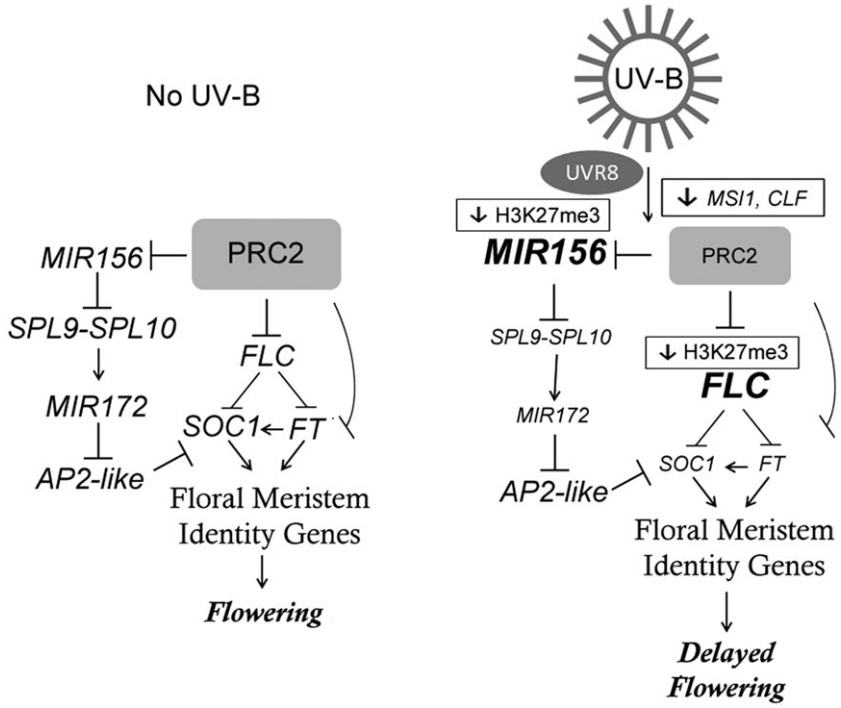

FIGURE 7 Flowering pathways involved in the UV-B mediated delay in flowering time in *Arabidopsis thaliana*. Left: gene regulatory networks without UV-B irradiation. The PRC2 complex regulates H3K27me3 deposition on *FLC*, *FT*, and *MIR156* genes inhibiting their expression. The age pathway involves the downregulation of *SPL* genes by miR156, including *SPL9* and *SPL10*, which in turn activate miR172 expression, a regulator of the flowering repressors *AP2*-like genes. Central to the autonomous and vernalization pathways, *FLC* represses the expression of the floral integrators *FT* and *SOC1*, which promote flowering after their expression reaches a threshold level. Right: A UVR8-mediated decrease in *CLF* and *MSI1* expression results in decreased H3K27me3 repressive mark at *MIR156* and *FLC*, increasing their expression in UV-B irradiated plants. A consequent decrease in the expression of components of the age pathway is observed, which together with an increase in *FLC* could explain the reduced accumulation of *SOC1* and *FT*, therefore resulting in a UV-B induced delay in flowering time. Positive interactions are represented with arrows, and negative interactions with bars; smaller fonts indicate decreased expression, and bigger fonts increased expression of the corresponding genes after UV-B exposure

of UVR8 action, regulating transcription of numerous downstream target genes, in several cases redundantly with HYH. Thus, although not proven in this manuscript, we hypothesize that mutants in *COP1*, *HY5*, and *HYH* should show similar flowering phenotypes after UV-B exposure as *uvr8* mutants. Our results open the question about the direct targets of UVR8 that are responsible for the downregulation of *CLF* and *MSI1*. It has been proposed that UV-B exposure of Arabidopsis plants increases acetylation of H3K9 and H3K14 at UVR8-regulated gene loci in a UVR8-dependent manner (Velanis, Herzyk, & Jenkins, 2016). One possibility is that one or more of these target genes that result actively transcribed through this UVR8-mediated acetylation mechanism may be negative regulators of *CLF* and *MSI1*.

Together, our study demonstrates that a daily exposure of Arabidopsis plants to UV-B radiation produces a delay in flowering time and this delay in flowering time requires UVR8 (Figure 7). We here provide details on the molecular mechanisms underlying this developmental reprogramming, which include downregulation of the expression of *MSI1* and *CLF*, two members of the PRC2 complex, resulting in a reduction in the methylation of H3K27 on the chromatin of key flowering regulators, leading to downregulation of the floral integrators. These changes occur mainly through the age pathway, producing an extended juvenile phase and a late flowering phenotype on UV-B irradiated Arabidopsis plants (Figure 7).

ACKNOWLEDGMENTS

We thank Dr. Julia Qüesta, Dr. Aman Husbands, Dr. Javier Palatnik, Dr. Nahuel González-Schain, Dr. Roman Ulm, and Dr. Scott Poethig for generously providing the seed stocks used in this work. This research was supported by Fondo para la Investigación Científica y Tecnológica grants PICT 2013-268 and 2015-157 to P. C.; P. C. and M. D. are members of the Researcher Career of the Consejo Nacional de Investigaciones Científicas y Técnicas (CONICET), and P. C. is an associate professor of UNR.

COMPETING INTERESTS

The authors declare that they have no competing interests.

ORCID

Paula Casati http://orcid.org/0000-0002-3194-4683

REFERENCES

Aukerman, M. J., & Sakai, H. (2003). Regulation of flowering time and floral organ identity by a MicroRNA and its APETALA2 -like target genes. *The Plant Cell*, *15*, 2730–2741.

Ausín, I., Alonso-Blanco, C., Jarillo, J. A., Ruiz-García, L., & Martínez-Zapater, J. M. (2004). Regulation of flowering time by FVE, a retinoblastoma-associated protein. *Nature Genetics*, *36*, 162–166.

Battey, N. H. (2000). Aspects of seasonality. *Journal of Experimental Botany*, *51*, 1769–1780.

Casadevall, R., Rodriguez, R. E., Debernardi, J. M., Palatnik, J. F., & Casati, P. (2013). Repression of growth regulating factors by the microRNA396 inhibits cell proliferation by UV-B radiation in Arabidopsis leaves. *The Plant Cell*, *25*, 3570–3583.

Casati, P. (2013). Analysis of UV-B regulated miRNAs and their targets in maize leaves. *Plant Signaling & Behavior*, *8*. e26758–e26751–6

Casati, P., Campi, M., Chu, F., Suzuki, N., Maltby, D., Guan, S., … Walbot, V. (2008). Histone acetylation and chromatin remodeling are required for UV-B – Dependent transcriptional activation of regulated genes in maize. *The Plant Cell*, *20*, 827–842.

Casati, P., & Walbot, V. (2003). Gene expression profiling in response to ultraviolet radiation in maize genotypes with varying. *Plant Physiology*, *132*, 1739–1754.

Cho, L.-H., Yoon, J., & An, G. (2016). The control of flowering time by environmental factors. *The Plant Journal*, *90*, 708–719.

De Lucia, F., Crevillen, P., Jones, A. M. E., Greb, T., & Dean, C. (2008). A PHD-polycomb repressive complex 2 triggers the epigenetic silencing of FLC during vernalization. *Proceedings of the National Academy of Sciences of the United States of America*, *105*, 16831–16836.

Demura, T., & Ye, Z.-H. (2010). Regulation of plant biomass production. *Current Opinion in Plant Biology*, *13*, 298–303.

Deng, W., Ying, H., Helliwell, C. A., Taylor, J. M., Peacock, W. J., & Dennis, E. S. (2011). FLOWERING LOCUS C (FLC) regulates development pathways throughout the life cycle of Arabidopsis. *Proceedings of the National Academy of Sciences of the United States of America*, *108*, 6680–6685.

Dotto, M., & Casati, P. (2017). Developmental reprogramming by UV-B radiation in plants. *Plant Science*, *264*, 96–101.

Favory, J.-J., Stec, A., Gruber, H., Rizzini, L., Oravecz, A., Funk, M., … Ulm, R. (2009). Interaction of COP1 and UVR8 regulates UV-B-induced photomorphogenesis and stress acclimation in Arabidopsis. *The EMBO Journal*, *28*, 591–601.

Frohnmeyer, H., & Staiger, D. (2003). Ultraviolet-B radiation-mediated responses in plants. Balancing damage and protection. *Plant Physiology*, *133*, 1420–1428.

Helliwell, C. A., Wood, C. C., Robertson, M., James, P. W., & Dennis, E. S. (2006). The Arabidopsis FLC protein interacts directly in vivo with SOC1 and FT chromatin and is part of a high-molecular-weight protein complex. *The Plant Journal*, *46*, 183–192.

Huijser, P., & Schmid, M. (2011). The control of developmental phase transitions in plants. *Development*, *138*, 4117–4129.

Hyun, Y., Richter, R., & Coupland, G. (2016). Competence to flower: Age-controlled sensitivity to environmental cues. *Plant Physiology*, *173*. 01523.2016

Jenkins, G. I. (2014). Structure and function of the UV-B photoreceptor UVR8. *Current Opinion in Structural Biology*, *29*, 52–57.

Jenkins, G. I. (2017). Photomorphogenic responses to ultraviolet-B light. *Plant, Cell and Environment*, *40*, 2544–2557.

Jiang, D., Wang, Y., Wang, Y., & He, Y. (2008). Repression of FLOWERING LOCUS C and FLOWERING LOCUS T by the Arabidopsis polycomb repressive complex 2 components. *PLoS One*, *3*. e3404–e3401–12

Jung, J. H., Seo, P. J., Kang, S. K., & Park, C. M. (2011). miR172 signals are incorporated into the miR156 signaling pathway at the SPL3/4/5 genes in Arabidopsis developmental transitions. *Plant Molecular Biology*, *76*, 35–45.

Klepikova, A. V., Logacheva, M. D., Dmitriev, S. E., & Penin, A. a. (2015). RNA-seq analysis of an apical meristem time series reveals a critical point in *Arabidopsis thaliana* flower initiation. *BMC Genomics*, *16*, 466.

Komeda, Y. (2004). Genetic regulation of time to flower in *Arabidopsis thaliana*. *Annual Review of Plant Biology*, *55*, 521–535.

Koornneef, M., Hanhart, C. J., & van der Veen, J. H. (1991). A genetic and physiological analysis of late flowering mutants in *Arabidopsis thaliana*. *Molecular & General Genetics*, *229*, 57–66.

Lopez-Vernaza, M., Yang, S., Müller, R., Thorpe, F., de Leau, E., & Goodrich, J. (2012). Antagonistic roles of SEPALLATA3, FT and FLC genes as targets of the polycomb group gene CURLY LEAF. *PLoS One*, *7*. e30715–e30711–10

Mackerness, S. A. (2000). Plant responses to ultraviolet-B (UV-B: 280-320 nm) stress: What are the key regulators? *Plant Growth Regulation*, *32*, 27–39.

Marquardt, S., Boss, P. K., Hadfield, J., & Dean, C. (2006). Additional targets of the Arabidopsis autonomous pathway members, FCA and FY. *Journal of Experimental Botany*, *57*, 3379–3386.

Michaels, S. D., & Amasino, R. M. (1999). FLOWERING LOCUS C encodes a novel MADS domain protein that acts as a repressor of flowering. *The Plant Cell*, *11*, 949–956.

Moon, J., Lee, H., Kim, M., & Lee, I. (2005). Analysis of flowering pathway integrators in Arabidopsis. *Plant and Cell Physiology*, *46*, 292–299.

Mutasa-Göttgens, E., & Hedden, P. (2009). Gibberellin as a factor in floral regulatory networks. *Journal of Experimental Botany*, *60*, 1979–1989.

Parihar, P., Singh, S., Singh, R., Singh, V. P., & Prasad, S. M. (2015). Changing scenario in plant UV-B research: UV-B from a generic stressor to a specific regulator. *Journal of Photochemistry and Photobiology B: Biology*, *153*, 334–343.

Perrella, G., & Kaiserli, E. (2016). Light behind the curtain: Photoregulation of nuclear architecture and chromatin dynamics in plants. *New Phytologist*, *212*, 908–919.

Questa, J., Song, J., Geraldo, N., An, H., & Dean, C. (2016). Arabidopsis transcriptional repressor VAL1 triggers polycomb silencing at FLC during vernalization. *Science*, *353*, 485–488.

Rajendiran, K., & Ramanujam, M. P. (2004). Improvement of biomass partitioning, flowering and yield by triadimefon in UV-B stressed *Vigna radiata* (L.) Wilczek. *Biologia Plantarum*, *48*, 145–148.

Rizzini, L., Favory, J.-J., Cloix, C., Faggionato, D., O'Hara, A., Kaiserli, E., … Ulm, R. (2011). Perception of UV-B by the Arabidopsis UVR8 protein. *Science*, *332*, 103–106.

Saile-Mark, M., & Tevini, M. (1997). Effects of solar UV-B radiation on growth, flowering and yield of central and southern European bush bean cultivars (Phaseolus vulgaris L.). In J. Rozema, W. W. C. Gieskes, S. C. Van De Geijn, C. Nolan, & H. De Boois (Eds.), *UV-B and biosphere* (pp. 114–125). Dordrecht: Springer Netherlands.

Salomé, P. A., Bomblies, K., Laitinen, R. A. E., Yant, L., & Mott, R. (2011). Genetic architecture of flowering time variation in *Arabidopsis thaliana*. *Genetics*, *188*, 421–433.

Schwarz, S., Grande, A. V., Bujdoso, N., Saedler, H., & Huijser, P. (2008). The microRNA regulated SBP-box genes SPL9 and SPL15 control shoot maturation in Arabidopsis. *Plant Molecular Biology*, *67*, 183–195.

Sheldon, C. C., Finnegan, E. J., Rouse, D. T., Tadege, M., Bagnall, D. J., Helliwell, C. A., … Dennis, E. S. (2000). The control of flowering by vernalization FRI. *Current Opinion in Plant Biology*, *3*, 418–422.

Shindo, C., Aranzana, M. J., Lister, C., Baxter, C., Nicholls, C., Nordborg, M., & Dean, C. (2005). Role of *FRIGIDA* and *FLOWERING LOCUS C* in determining variation in flowering time of Arabidopsis. *Plant Physiology*, *138*, 1163–1173.

Simpson, G. G. (2004). The autonomous pathway: Epigenetic and post-transcriptional gene regulation in the control of Arabidopsis flowering time. *Current Opinion in Plant Biology*, *7*, 570–574.

Spanudakis, E., & Jackson, S. (2014). The role of microRNAs in the control of flowering time. *Journal of Experimental Botany*, *65*, 365–380.

Steinbach, Y., & Hennig, L. (2014). Arabidopsis MSI1 functions in photoperiodic flowering time control. *Frontiers in Plant Science*, *5*, 77.

Tooke, F., Ordidge, M., Chiurugwi, T., & Battey, N. (2005). Mechanisms and function of flower and inflorescence reversion. *Journal of Experimental Botany*, *56*, 2587–2599.

Ulm, R., Baumann, A., Oravecz, A., Máté, Z., Adám, E., Oakeley, E. J., … Nagy, F. (2004). Genome-wide analysis of gene expression reveals function of the bZIP transcription factor HY5 in the UV-B response of Arabidopsis. *Proceedings of the National Academy of Sciences of the United States of America*, *101*, 1397–1402.

Vanhaelewyn, L., Prinsen, E., Van Der Straeten, D., & Vandenbussche, F. (2016). Hormone-controlled UV-B responses in plants. *Journal of Experimental Botany*, *67*, 4469–4482.

Varkonyi-Gasic, E., Wu, R., Wood, M., Walton, E. F., & Hellens, R. P. (2007). Protocol: A highly sensitive RT-PCR method for detection and quantification of microRNAs. *Plant Methods*, *3*, 12.

Velanis, C. N., Herzyk, P., & Jenkins, G. I. (2016). Regulation of transcription by the Arabidopsis UVR8 photoreceptor involves a specific histone modification. *Plant Molecular Biology*, *92*, 425–443.

Wang, J. W. (2014). Regulation of flowering time by the miR156-mediated age pathway. *Journal of Experimental Botany*, *65*, 4723–4730.

Wang, J. W., Czech, B., & Weigel, D. (2009). miR156-regulated SPL transcription factors define an endogenous flowering pathway in *Arabidopsis thaliana*. *Cell*, *138*, 738–749.

Wu, S.-H. (2014). Gene expression regulation in photomorphogenesis from the perspective of the central dogma. *Annual Review of Plant Biology*, *65*, 311–333.

Wu, G., Park, M. Y., Conway, S. R., Wang, J. W., Weigel, D., & Poethig, R. S. (2009). The sequential action of miR156 and miR172 regulates developmental timing in Arabidopsis. *Cell*, *138*, 750–759.

Wu, G., & Poethig, R. S. (2006). Temporal regulation of shoot development in *Arabidopsis thaliana* by miR156 and its target SPL3. *Development*, *133*, 3539–3547.

Xu, M., Hu, T., Smith, M. R., & Poethig, R. S. (2015). Epigenetic regulation of vegetative phase change in Arabidopsis. *The Plant Cell*, *28*, TPC2015-00854-RA.

Xu, M., Hu, T., Zhao, J., Park, M.-Y., Earley, K. W., Wu, G., … Poethig, R. S. (2016). Developmental functions of miR156-regulated SQUAMOSA PROMOTER BINDING PROTEIN-LIKE (SPL) genes in *Arabidopsis thaliana*. *PLoS Genetics*, *12*, e1006263.

Yu, C.-W., Chang, K., & Wu, K. (2016). Genome-wide analysis of gene regulatory networks of the FVE-HDA6-FLD complex in Arabidopsis. *Frontiers in Plant Science*, *7*, 1–13.

SUPPORTING INFORMATION

Additional Supporting Information may be found online in the supporting information tab for this article.

Figure S1. Effect of UV-B light on flowering time under short day conditions. (a) Number of rosette leaves in control plants compared to UV-B irradiated plants. Values represented are mean ± SD for 10 plants (Student's t-test, * = $p < 0.05$). (b) Picture of plants grown under white light supplemented with UV-B light, which flower later than control plants.

Figure S2. Relative expression of *SWN* in control and UV-B irradiated plants. Analysis by qRT-PCR was performed at 9, 12 and 25 days of growth. Transcript levels in UV-B treated plants normalized to untreated control plants are shown (mean ± SD; * = $p < 0.05$).

Figure S3: Changes in expression of flowering genes in *clf-29* mutant plants. (a) Normalized expression of *FLC*, *FT* and *SOC1* in Col-0 and *clf-29* plants. (b) Normalized expression of *FLC*, *FT* and *SOC1* in control and UV-B irradiated *clf-29* plants. Analyzed by qRT-PCR at 12 days of growth. Transcript levels normalized to reference gene are shown (mean ± SD; * = $p < 0.05$; ** = $p < 0.001$).

Figure S4. Days before flowering of control and UV-B treated for *se-1* and *hyl1-2* mutant plants. Values represented are mean ± SD for at least 10 plants (Student's t-test, * = $p < 0.05$; ** = $p < 0.01$).

Table S1. Primers used in this work.

Table S2. Effect of UV-B radiation on flowering time of mutant lines

How to cite this article: Dotto M, Gómez MS, Soto MS, Casati P. UV-B radiation delays flowering time through changes in the PRC2 complex activity and miR156 levels in *Arabidopsis thaliana*. *Plant Cell Environ*. 2018;1–13. https://doi.org/10.1111/pce.13166